Regulation of skeletal muscle lipolysis and oxidative metabolism by the co-lipase CGI-58[s]

Pierre-Marie Badin,[1,]* Camille Loubière,[1,]* Maarten Coonen,* Katie Louche,* Geneviève Tavernier,* Virginie Bourlier,* Aline Mairal,* Arild C. Rustan,[†] Steven R. Smith,[§] Dominique Langin,* and Cedric Moro[2,]*

Inserm, 1048,* Obesity Research Laboratory, Institute of Metabolic and Cardiovascular Diseases, Paul Sabatier University, Toulouse, France; Department of Pharmaceutical Biosciences,[†] School of Pharmacy, University of Oslo, Oslo, Norway; and Translational Research Institute for Metabolism and Diabetes,[§] Florida Hospital and the Burnham Institute for Medical Research, Winter Park, FL

Abstract We investigated here the specific role of CGI-58 in the regulation of energy metabolism in skeletal muscle. We first examined CGI-58 protein expression in various muscle types in mice, and next modulated CGI-58 expression during overexpression and knockdown studies in human primary myotubes and evaluated the consequences on oxidative metabolism. We observed a preferential expression of CGI-58 in oxidative muscles in mice consistent with triacylglycerol hydrolase activity. We next showed by pulse-chase that CGI-58 overexpression increased by more than 2-fold the rate of triacylglycerol (TAG) hydrolysis, as well as TAG-derived fatty acid (FA) release and oxidation. Oppositely, CGI-58 silencing reduced TAG hydrolysis and TAG-derived FA release and oxidation (-77%, $P < 0.001$), whereas it increased glucose oxidation and glycogen synthesis. Interestingly, modulations of CGI-58 expression and FA release are reflected by changes in pyruvate dehydrogenase kinase 4 gene expression. This regulation involves the activation of the peroxisome proliferator activating receptor-δ (PPARδ) by lipolysis products.[JLR] Altogether, these data reveal that CGI-58 plays a limiting role in the control of oxidative metabolism by modulating FA availability and the expression of PPARδ-target genes, and highlight an important metabolic function of CGI-58 in skeletal muscle.—Badin, P-M., C. Loubière, M. Coonen, K. Louche, G. Tavernier, V. Bourlier, A. Mairal, A. C. Rustan, S. R. Smith, D. Langin, and C. Moro. Regulation of skeletal muscle lipolysis and oxidative metabolism by the co-lipase CGI-58. *J. Lipid Res.* 2012. 53: 839–848.

Supplementary key words comparative gene identification 58 • fatty acid • substrate oxidation • intramyocellular triacylglycerol • peroxisome proliferator-activated receptor • mitochondria

Adipose triglyceride lipase (ATGL) is a novel adipose-enriched lipase that mediates the initial step in triacylglycerol (TAG) hydrolysis in various tissues of the body (1, 2). It was shown by Lass et al. (3) that ATGL activity is regulated by the product of the CGI-58 gene (comparative gene identification 58). Loss-of-function mutations in the human CGI-58 gene are sufficient to promote excessive lipid accumulation in most tissues leading to neutral lipid storage disease with ichtyosis (4). This clinical phenotype is more inconsistently associated with skeletal and cardiac myopathy, liver steatosis and hepatosplenomegaly as recently reviewed (5). CGI-58 mutant proteins are unable to induce ATGL activity, which results in cellular lipid accumulation in the form of TAG (3). Of interest, recent work indicates that the rate-limiting step for the mobilization of intracellular TAG is the release of CGI-58 from specific lipid droplet scaffold proteins such as Perilipin-A (6). Together, these data suggest that CGI-58 may be important for the control of lipolysis in several tissues.

Previous studies had shown the role of hormone sensitive lipase (HSL) in the regulation of intramyocellular TAG (IMTG) during exercise in humans (7, 8). However, HSL deficiency does not affect IMTG in skeletal muscle (9, 10). ATGL was recently shown to be expressed in human skeletal muscle predominantly in type I oxidative fibers (11). Thus, ATGL-deficient mice exhibit a defective TAG hydrolase activity in skeletal muscle and accumulate large amount of TAG in various tissues (1). These data suggest that ATGL may play an important role in the regulation of IMTG and lipolysis notably in skeletal muscle.

Furthermore, elevated ATGL activity and/or expression in human skeletal muscle was shown to play a role in the development of insulin resistance, a major risk factor for the development of type 2 diabetes (12). However, the regulation of ATGL activity in human skeletal muscle is currently poorly documented. We hypothesized that CGI-58 could be a critical regulator of human skeletal muscle TAG metabolism and substrate oxidation. The aim of the study was to examine the functional role of CGI-58 in human skeletal muscle by gain- and loss-of-function studies. We next measured the impact of elevated or reduced levels of CGI-58 on energy metabolism, mitochondrial activity, and gene expression in cultured human primary myotubes.

MATERIALS AND METHODS

Subjects

Six young healthy subjects, mean age 22.9 ± 0.4 yrs (18–29) and mean BMI 26.5 ± 0.5 kg/m^2 (20.1–34.7) were recruited in the study. The protocol was approved by the institutional review board of the Pennington Biomedical Research Center, and all volunteers gave written informed consent. The participants were asked to refrain from vigorous physical activity for 48 h before presenting to the Pennington inpatient clinic, and ate a weight-maintaining diet consisting of 35% fat, 16% protein, and 49% carbohydrate 2 days before the muscle biopsy. Samples of *vastus lateralis* weighing 60–100 mg were obtained using the Bergstrom technique, blotted, cleaned, and snap-frozen in liquid nitrogen (13). Human subcutaneous adipose tissue was obtained from six moderately overweight women undergoing plastic surgery. Their mean age was 44.6 ± 2.9 years and their mean BMI was 27.5 ± 1.2 kg/m^2. The study was in agreement with the Declaration of Helsinki, and the French National Institute of Health and Medical Research (INSERM) and the Toulouse University Hospital ethics regulation.

Animals

All experimental procedures were approved by a local ethical committee and performed according to INSERM animal core facility guidelines for the care and use of laboratory animals. Four- to five-week-old C57Bl/6 mice were housed in a pathogen-free barrier facility (12 h light/dark cycle) and fed a standard laboratory chow diet (D12450B) for 4 weeks before euthanasia and tissue collection.

Skeletal muscle cell culture

Satellite cells from *rectus abdominis* of healthy subjects (age 34.3 ± 2.5 years, BMI 26.0 ± 1.4 kg/m^2, fasting glucose 5.0 ± 0.2 mM) were isolated by trypsin digestion, preplated on an uncoated petri dish for 1 h to remove fibroblasts, and subsequently transferred to T-25 collagen-coated flasks in DMEM supplemented with 10% FBS and growth factors (human epidermal growth factor, BSA, dexamethasone, gentamycin, fungizone, fetuin) as previously described (12, 14). Cells were grown at 37°C in a humidified atmosphere of 5% CO_2. Differentiation of myoblasts into myotubes was initiated at ~80-90% confluence, by switching to α-MEM with antibiotics, 2% FBS, and fetuin. The medium was changed every other day and cells were grown up to 5 days.

Overexpression and knockdown studies

Human adipose tissue CGI-58 cDNA (Fwd: GCGGCTATGGCG-GCGGAGGAGGA; Rev: GTGTTCAGTCCACAGTGTCGCAGAT)

was cloned into the pcDNA3 vector (InVitrogen Corp., Carlsbad, CA). DNA sequencing was performed to check correct insertion of the cDNA using an ABI3100 automatic sequencer (Applied Biosystems, Courtaboeuf, France). For overexpression experiments, adenoviruses expressing bicistronic vectors containing in tandem GFP and hCGI-58 were constructed, purified, and titrated (Vector Biolabs, Philadelphia, PA). An adenovirus containing the GFP gene only was used as a control. Myotubes were infected with the control and hCGI-58 adenoviruses at day 4 of differentiation and remained exposed to the virus for 24 h in serum-free DMEM containing 150 μM of oleate complexed to BSA (ratio 4/1). For knockdown studies, lentiviral particles encoding for a shRNA of hCGI-58 (Sigma-Aldrich, France) or a scramble control (nontarget) were exposed for 24 h to the culture at the beginning of the differentiation. Infection efficiency was assessed using a TurboGFP control. Oleate was preferred to palmitate for lipid loading of the cells, to favor TAG synthesis and to avoid the intrinsic lipotoxic effect of palmitate (15, 16). No adenovirus-induced cellular toxicity was observed as determined by chemiluminescent quantification of adenylate kinase activity (ToxiLight, Lonza Group Ltd, Basel, Switzerland).

Determination of FA metabolism

Cells were pulsed overnight for 18 h with [1-^{14}C]oleate (1 μCi/ml; PerkinElmer, Boston, MA) and cold oleate (80 μM), to prelabel the endogenous TAG pool. Oleate was coupled to FA-free BSA in a molar ratio of 5:1. Some cells were harvested at the end of the pulse for the 0 time point. Following the pulse, myotubes were chased for 1, 3, and 6 h in DMEM containing 0.1 mM glucose, 0.5% FA-free BSA, and 10 μM triacsin C to block FA recycling into the TAG pool as described elsewhere (17, 18). TAG-derived FA oxidation (endogenous FA oxidation) measured by the sum of $^{14}CO_2$ and ^{14}C-ASM (acid soluble metabolites) was measured in absence of triacsin C as previously described (14). Myotubes were harvested in 0.2 ml SDS 0.1% at the end of the pulse and of the chase period to determine oleate incorporation into TAG, DAG, MAG (monoacylglycerol), FA, and protein content. The lipid extract was separated by TLC using heptane-isopropylether-acetic acid (60:40:4, v/v/v) as developing solvent. All assays were performed in duplicates, and data were normalized to cell protein content.

Determination of glucose metabolism

Cells were preincubated with a glucose- and serum-free medium for 90 min then exposed to DMEM supplemented with D[U-^{14}C]glucose (1 μCi/ml; PerkinElmer, Boston, MA) in the presence or absence of 100 nM insulin (Humulin®) for 3 h. Following incubation, glucose oxidation, and glycogen synthesis were determined as previously described (12).

Western blot analysis

Muscle tissues and cell extracts were homogenized in a buffer containing 50 mM HEPES, pH 7.4, 2 mM EDTA, 150 mM NaCl, 30 mM NaPPO4, 10 mM NaF, 1% Triton X-100, 10 μl/ml protease inhibitor (Sigma-Aldrich), 10 μl/ml phosphatase I inhibitor (Sigma-Aldrich), 10 μl/ml phosphatase II inhibitor (Sigma-Aldrich), and 1.5 mg/ml benzamidine HCl. Tissue homogenates were centrifuged for 25 min at 15,000 g and supernatants were stored at −80°C. Solubilized proteins from muscle tissue and myotubes were run on a 4-12% SDS-PAGE (Biorad), transferred onto nitrocellulose membrane (Hybond ECL, Amersham Biosciences), and incubated with the primary antibody CGI-58, (Abnova Corp., Tapei, Taiwan), PDK4 (Abnova), pAMPK, and AMPK (Cell Signaling Technology Inc., Beverly, MA). Subsequently, immunoreactive proteins were determined by enhanced chemiluminescence

reagent (GE Healthcare) and visualized by exposure to Hyperfilm ECL (GE Healthcare). GAPDH (Cell Signaling Technology) served as an internal control.

Lipase activity assays

Triacylglycerol hydrolase (TAGH) activity was measured on tissue and cell lysates as previously described (19). Briefly, tissue and cell lysates were extracted in a lysis buffer containing 0.25 M sucrose, 1 mM EDTA, 1 mM DTT, 20 μg/ml leupeptin, and 2 μg/ml anti-pain. [9, 10-^{3}H(N)]triolein and cold triolein were emulsified with phospholipids by sonication. The emulsion was incubated for 30 min at 37°C in the presence of 10–40 μg of total protein from tissue and cell lysates. After incubation, the reaction was terminated by adding 3.25 ml of methanol-chloroform-heptane (10:9:7) and 1 ml of 0.1 M potassium carbonate, 0.1 M boric acid, (pH 10.5). After centrifugation (800 g, 15 min), 0.5 ml of the upper phase was collected for scintillation counting. Stimulation of ATGL was achieved by coincubation of tissue lysates with 1.6 μg of recombinant human CGI-58 (rhCGI-58) (Abnova). The data are expressed in nmol of oleic acid released $\cdot$ min^{-1} $\cdot$ mg^{-1} of protein.

TAG determination by GC-MS

Total lipids were extracted from frozen muscle tissue samples and from myotubes harvested in water containing 0.25 ml 0.1% SDS. Lipids were extracted using the method of Folch et al. (20). The extracts were filtered and lipids recovered in the chloroform phase. TAGs were isolated using TLC on Silica Gel 60 A plates developed in petroleum ether- ethyl ether- acetic acid (80:20:1) and visualized by rhodamine 6G. The TAG band was scraped from the plate and methylated using BF$_3$/methanol as described by Morrison and Smith (21). The methylated fatty acids were extracted with hexane and analyzed by GC using an HP 5890 gas chromatograph equipped with flame ionization detectors, an HP 3365 Chemstation, and a capillary column (SP2380, 0.25 mm × 30 m, 0.25 μm film, Supelco, Bellefonte, PA). Helium was used as a carrier gas. The oven temperature was programmed from 160°C to 230°C at 4°C/min. Fatty acid methyl esters were identified by comparing the retention times to those of known standards. Inclusion of the internal standards, 20:1 (trieicosenoin) and 17:0 (diheptadecanoin), permits quantitation of the amount of TAG in the sample.

Determination of mitochondrial content

For quantification of mitochondrial content, we measured the mitochondrial (mt) to nuclear DNA ratio as previously described (22). The sequences for the primer sets used for determination of mtDNA for NADH dehydrogenase subunit 1 (ND1) were forward primer CCCTAAAACCCGCCACATCT, reverse primer GAGCGAT-GGTGAGAGCTAAGGT, and of nuclear DNA for lipoprotein lipase (LPL) were forward primer CGAGTCGTCTTTCTCCTGATGAT, reverse primer TTCTGGATTCCAATGCTTCGA. We also determined mitochondrial mass in myotubes using Mitotracker Green FM (Invitrogen, Carlsbad, CA), which stains mitochondrial matrix protein irrespective of the membrane potential and thus provides an accurate assessment of mitochondrial mass. Similarly, we measured mitochondrial membrane potential using a Mitotracker Red CMX-Ros (Invitrogen), which stains mitochondria according to their membrane potential. Briefly, cells were washed with 1× PBS and incubated at 37°C for 30 min with 100 nM of each Mitotracker. Cells were then harvested using trypsin/EDTA and resuspended in 1× PBS. Fluorescence intensity was measured on a fluorometer and values corrected for total protein.

Real-time qRT-PCR

Total RNA from cultured myotubes was isolated in RNeasy Lysis Buffer + β-mercaptoethanol reagent (Qiagen GmbH, Hilden, Germany). The quantity of the RNA was determined on a Nanodrop ND-1000 (Thermo Scientific, Rockford, IL, USA). Reverse-transcriptase PCR was performed on a GeneAmp PCR System 9700 using the Multiscribe Reverse Transcriptase method (Applied Biosystems, Foster City, CA). Real-time quantitative PCR (qPCR) was performed to determine cDNA content. All primers were bought from Applied Biosystems. Primers used were: 18S (Taqman assay ID: Hs99999901_s1), PDK4 (Hs01037712_m1), GLUT4 (Hs00168966_m1), HSL (Hs00193510_m1), MYH1 (Hs00428600_m1). qPCR was then performed on a StepOnePLus real-time PCR system (Applied Biosystems). For each primer, a standard curve was made prior to mRNA quantification to assess the optimal total cDNA quantity. All expression data were normalized by the $2^{(\Delta\Delta Ct)}$ method using 18S as internal control.

Statistical analyses

All statistical analyses were performed using GraphPad Prism 5.0 for Windows (GraphPad Software Inc., San Diego, CA). One-way ANOVA followed by Tukey's posthoc tests were applied in time-course studies and paired Student's t-tests were performed to determine differences between treatments. Two-way ANOVA and Bonferroni's posthoc tests were used when appropriate. All values in figures and tables are presented as mean ± SEM. Statistical significance was set at $p < 0.05$.

RESULTS

CGI-58 expression and triglyceride hydrolase activity in different muscle types

We examined CGI-58 protein expression by western blot in various types of muscle in mice. The data show that CGI-58 is quantitatively more abundant in oxidative muscles. The expression pattern is as follow: heart>*soleus*>quadriceps>white *gastrocnemius* (**Fig. 1A**). This pattern was somehow consistent with the TAGH activity pattern observed in these muscles. TAGH activity was highest in heart and *soleus* when compared with quadriceps and *gastrocnemius* (Fig. 1B). TAGH activity was about 5 times lower in *soleus* and heart when compared with epidydimal white adipose tissue ($P < 0.001$). We next investigated the ability of human recombinant CGI-58 (rhCGI-58) to induce TAGH activity (TAGH) in human adipose tissue (AT) and skeletal muscle (SkM) lysates (Fig. 1C). Exogenous rhCGI-58 almost doubled TAGH activity in hSkM (1.8-fold, $P = 0.004$) but did not induce TAGH activity in hAT. The validity of the system was checked by the ability of rhCGI-58 to induce TAGH activity in COS7 cell lysates stably overexpressing hATGL (8-fold, $P < 0.01$).

Overexpression of CGI-58 in human primary myotubes

Adenovirus-mediated overexpression of hCGI-58 led to a 2-fold increase in CGI-58 protein content in 5 day differentiated human myotubes ($P < 0.05$) (**Fig. 2A**). The adenovirus infection efficiency averaged 50% (GFP-positive myotubes to DAPI ratio) and was comparable between control (Ad-GFP) and Ad-CGI-58 (data not shown). Surprisingly, CGI-58 overexpression was paralleled by a downregulation of ATGL protein (-34%, $P < 0.05$) (Fig. 2B). As expected, CGI-58 overexpression increased TAGH activity (2-fold, $P < 0.05$) (Fig. 2C) and reduced total TAG content (-51%, $P < 0.01$) (Fig. 2D).
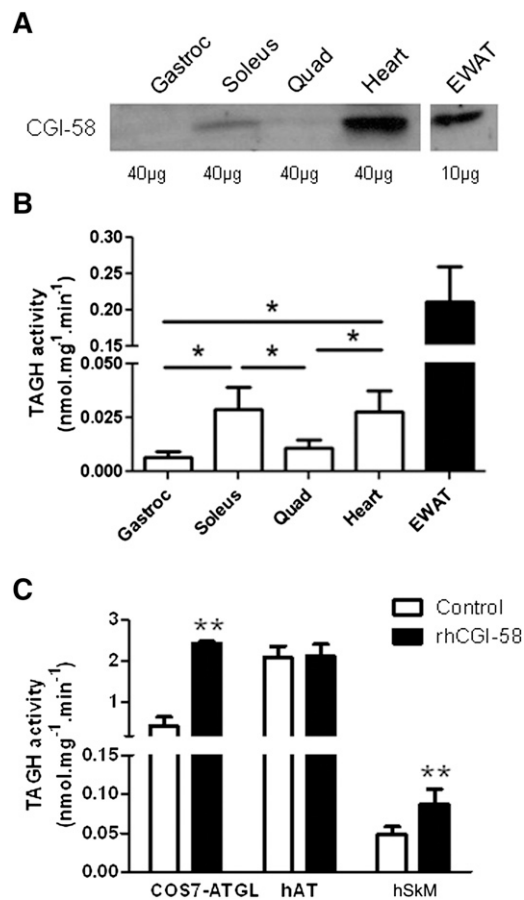
Fig. 1. Distribution and function of CGI-58 in skeletal muscle. A: Representative blot of CGI-58 protein expression in different types of muscle and EWAT [whole *gastrocnemius* (gastroc), *soleus*, quadriceps (quad) and heart, as well as epididimal white adipose tissue] in 20-week-old mice. Forty micrograms of total protein were loaded for the different muscles and 10 μg for EWAT (n = 3). B: Triacylglycerol hydrolase activity (TAGH) was measured in different types of muscle and EWAT in 20-week-old mice as previously (n = 6), One-way ANOVA * $P < 0.05$. C: TAGH was measured in human adipose tissue (hAT) and skeletal muscle (hSkM) in absence (control) or presence of recombinant human CGI-58 (rhCGI-58) (n = 6). A positive control experiment was performed in presence of COS7 cell extracts overexpressing human ATGL (COS7/ATGL), paired Student's *t*-test ** $P < 0.01$ when compared with control.

Impact of CGI-58 overexpression on lipolysis and FA oxidation

We performed pulse-chase experiments to evaluate the role of CGI-58 in the regulation of intracellular TAG hydrolysis and FA metabolism. Chase experiments were performed in the presence of 10 μM of triacsin C, which blocks 99.4% of TAG and 95.5% of DAG synthesis during 24 h loading with radiolabeled oleate in human primary myotubes (supplementary Fig. I). Endogenous TAGs were prelabeled with [1-^{14}C]oleate and subsequently, TAG hydrolysis and FA release into the culture medium were determined in GFP and CGI-58 overexpressing myotubes at different time points (**Fig. 3**). TAG depletion was increased at different time points in CGI-58 overexpressing myotubes compared with GFP controls (Fig. 3A). Consistent with an increased TAG hydrolysis, FA release into the medium was higher in CGI-58 overexpressing myotubes

during the chase period (Fig. 3B). Of interest, CGI-58 overexpression increased the oxidation of endogenous FA originating from the TAG pool (2.2-fold, $P < 0.05$) (Fig. 3C). In line with an increased TAG hydrolysis, radiolabeled oleate incorporation into DAG, MAG, and intracellular FA was strongly upregulated in CGI-58 overexpressing myotubes (supplementary Fig. II A–C). Thus, because CGI-58 was reported to display a significant lysophosphaditic acid acyltransferase (LPAAT) activity (23, 24), we could show a robust increase in phospholipid synthesis in CGI-58 overexpressing myotubes (supplementary Fig. II D).

## Impact of CGI-58 knockdown on lipolysis and FA oxidation

We used a lentiviral vector to knock down CGI-58 in differentiated myotubes and achieved 89% reduction of CGI-58 protein expression ($P < 0.01$) (**Fig. 4A**). Interestingly, CGI-58 knockdown induced important changes in neutral lipid dynamics and FA metabolism. CGI-58 knockdown robustly reduced TAG hydrolysis and protected endogenous TAG pools from lipolysis when compared with control (Fig. 4B). Consistently, FA release into the culture medium was significantly reduced (Fig. 4C), as well as the appearance of DAG, MAG, and intracellular FA consecutive to lipolysis (supplementary Fig. III A–C). The changes in FA release were paralleled by a robust drop in intracellular TAG-derived FA oxidation (-77%, $P < 0.001$) reflecting endogenous FA oxidation (Fig. 4D). As previously, phospholipid synthesis was slightly reduced (supplementary Fig. III D), suggesting that CGI-58 contributes to some extent to total skeletal muscle LPAAT activity.

Effects of CGI-58 knockdown on mitochondria

In light of the robust suppression of TAG-derived FA oxidation beyond the decrease of FA release from lipolysis, we sought to investigate whether modulations of CGI-58 expression alter mitochondrial activity. We first examined mitochondrial content using Mitotracker green, which stains mitochondrial matrix protein independently of the mitochondrial membrane potential and mainly reflects mitochondrial mass. We could show that mitochondrial mass is similar between control and siCGI-58 myotubes (**Fig. 5A**) and confirmed these results by the measure of the mitochondrial-to-nuclear DNA ratio (1.516 ± 0.008 vs. 1.540 ± 0.009 A.U. for control and siCGI-58 respectively, NS). Interestingly, mitochondrial membrane potential measured by fluorescence staining was reduced by 27% ($P = 0.016$) in siCGI-58 myotubes (Fig. 5B). This drop in membrane potential was paralleled by a 70% increase of the cellular energy-sensor AMPK phosphorylation state (pAMPK to AMPK ratio) despite a decrease in total AMPK protein content in siCGI-58 myotubes (-50%, $P < 0.05$) (Fig. 5C).

## Effects of CGI-58 knockdown on glucose metabolism

We next evaluated the consequences of CGI-58 knockdown on glucose metabolism. Importantly, we observed a higher glucose oxidation in siCGI-58 myotubes (**Fig. 6A**), paralleled by an increased glucose incorporation into glycogen in the basal state and upon insulin stimulation (Fig. 6B).
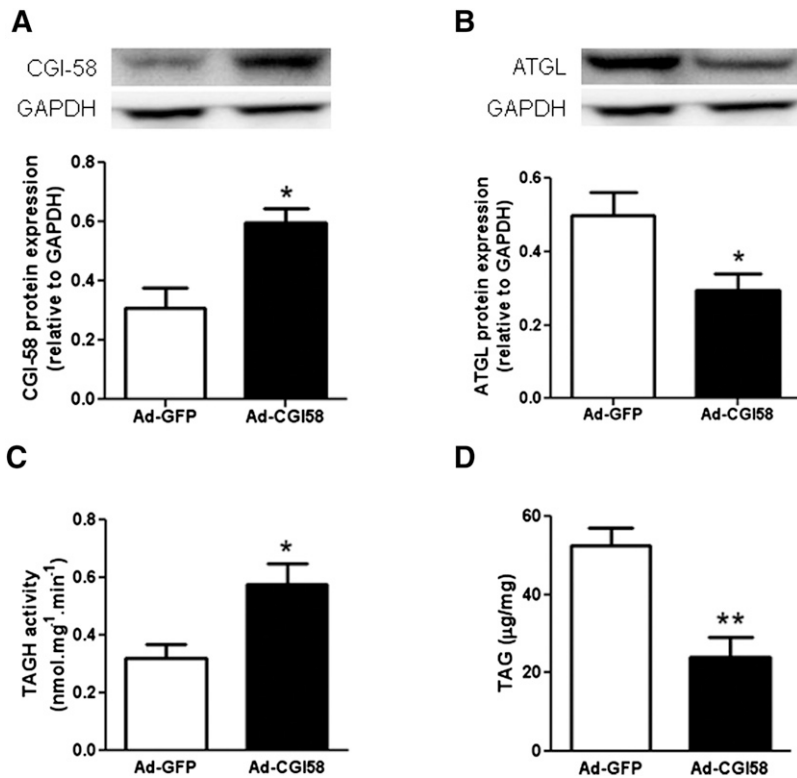
Fig. 2. CGI-58 overexpression promotes TAG breakdown. A: CGI-58 and (B) ATGL protein content were measured in control myotubes (Ad-GFP) and myotubes overexpressing CGI-58 (Ad-CGI58) (n = 5). Insets are showing representative blots and loading control of each protein, * $P < 0.05$ versus Ad-GFP. C: TAGH activity and (D) total TAG content were measured in control myotubes (Ad-GFP) and myotubes overexpressing CGI-58 (Ad-CGI58) (n = 5), paired Student's *t*-test * $P < 0.05$, ** $P < 0.01$ versus Ad-GFP.

To gain insight into the mechanism contributing to the substrate switch, we measured pyruvate dehydrogenase kinase 4 (PDK4) expression. PDK4 is a mitochondrial protein that inhibits the pyruvate dehydrogenase complex by phosphorylating one of its subunits, thereby inhibiting glucose oxidation (25). The data show that PDK4 protein expression was very significantly reduced by 41% in siCGI-58 myotubes (Fig. 6C). The downregulation of PDK4
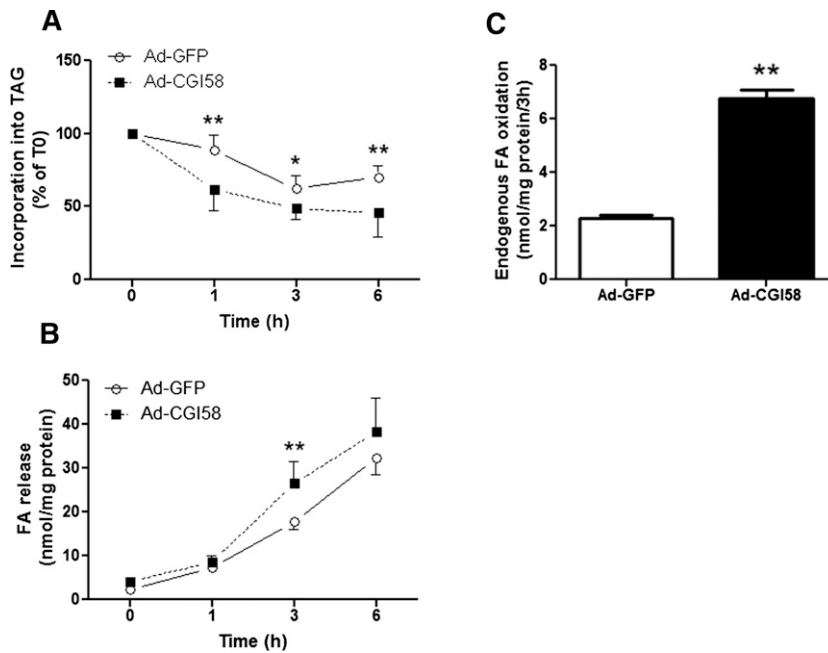
Fig. 3. CGI-58 increases TAG-derived FA release and oxidation. Pulse-chase experiments were performed to determine the time-course over 6 h of (A) TAG hydrolysis and (B) FA release into the culture medium, in control myotubes (Ad-GFP) and myotubes overexpressing CGI-58 (Ad-CGI58) (n = 6). TAG content was expressed as a function of the value at the 0 time point (% of T0). All parameters were measured at the end of the Pulse (0 time point) and during the Chase period (1, 3, and 6 h time points). Two-way ANOVA * $P < 0.05$, ** $P < 0.01$ when compared with Ad-GFP. C: Endogenous oxidation, i.e., TAG-derived FA oxidation was measured in absence of triacsin C after 3 h of Chase in the same conditions. Paired Student's *t*-test ** $P < 0.01$ when compared with Ad-GFP.
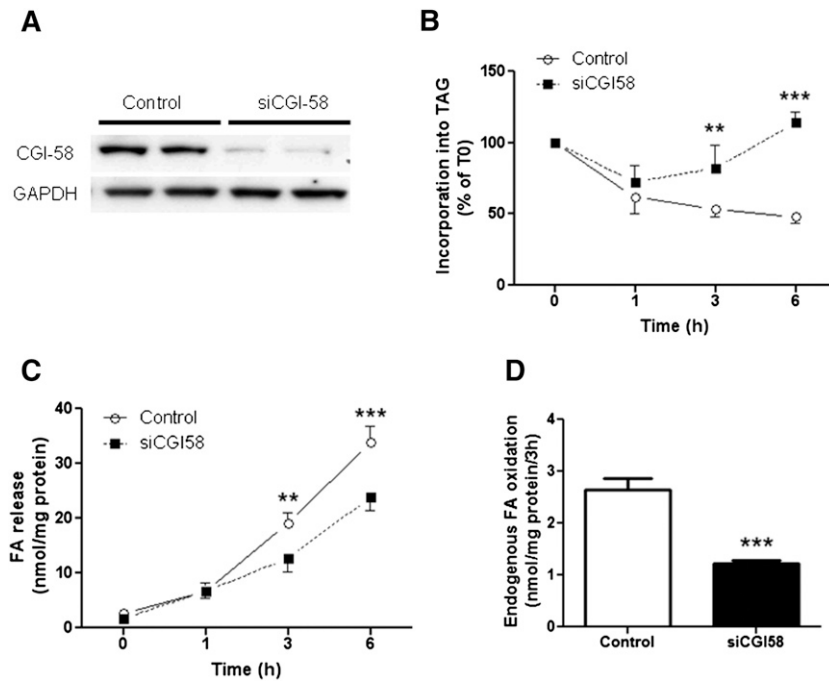
Fig. 4. CGI-58 silencing reduces lipolysis and TAG-derived FA oxidation. A: Representative blot of CGI-58 protein expression in control myotubes and myotubes knocked down for CGI-58 (siCGI58) (n = 2 lane per condition). We next measured by pulse-chase the time-course over 6 h of (B) TAG hydrolysis, (C) FA release into the culture medium in control myotubes and myotubes knocked down for CGI-58 (siCGI58) (n = 6). All parameters were measured at the end of the Pulse (0 time point) and during the Chase period (1, 3, and 6 h time points). TAG content was expressed as a function of the value at the 0 time point (% of T0). Two-way ANOVA ** $P < 0.01$, *** $P < 0.0001$ when compared with control. D: Endogenous oxidation, i.e., TAG-derived FA oxidation, was measured in absence of triacsin C after 3 h of Chase in the same conditions. Paired Student's t-test *** $P < 0.0001$ when compared with control.

was also observed at the mRNA level reflecting transcriptional modulations of the gene.

Modulations of CGI-58 and PPARδ target-genes

Because PDK4 has been described as a PPARδ-target gene (26), we examined the level of expression of several known PPARδ-target genes among other genes in skeletal muscle. We found that CGI-58 knockdown was associated with the downregulation of known PPARδ-target genes such as PDK4, GLUT4, HSL, and MYH1 gene expression (data not shown). Importantly, we validated that PDK4 gene expression was induced by a selective PPARδ agonist (GW0742) and efficiently blocked by a selective PPARδ antagonist (GSK0660) (**Fig. 7A**). We further show that PDK4 gene expression is strongly induced by oleate (Fig. 7B). This induction was almost completely abolished in presence of the selective PPARδ antagonist GSK0660. Thus, we also show that a selective PPARα agonist (GW7647) failed to induce PDK4 gene expression in human skeletal muscle cells. Interestingly, we next showed that CGI-58 overexpression was accompanied by an upregulation of PDK4 gene expression that was totally blunted by the PPARδ antagonist (Fig. 7C). Reciprocally, we observed a significant suppression of PDK4 mRNA level in myotubes invalidated for CGI-58 that was totally rescued by the selective PPARδ agonist (Fig. 7D).

DISCUSSION

Obesity and type 2 diabetes are associated with ectopic lipid deposition in insulin-sensitive tissue such as skeletal muscle (27, 28). The understanding of the regulation of IMTG metabolism has gained much interest because IMTG content inversely correlates with peripheral insulin sensitivity (19, 29–31). In this study, we identify that the ATGL coactivator CGI-58 has a master regulator of human skeletal muscle TAG metabolism. We first show that CGI-58 is mostly expressed in oxidative muscles (*soleus* and heart) where it coactivates ATGL to increase TAGH activity. Importantly, we demonstrate that CGI-58 is a limiting factor of skeletal muscle TAG metabolism and IMTG-derived FA oxidation. Thus, we also show that CGI-58 modulates skeletal muscle gene expression by regulating the availability of PPARδ FA ligands.

We identified a preferential expression of CGI-58 in oxidative muscle (heart and *soleus*) when compared with more glycolytic muscle (quadriceps and *gastrocnemius*). The highest expression was found in the heart. These findings are consistent with the strong TAGH activity predominantly observed in oxidative muscles in agreement with earlier studies (32). This result implies that CGI-58 may be mainly expressed in type I oxidative fibers as recently noted for ATGL (11). We further demonstrate that rhCGI-58
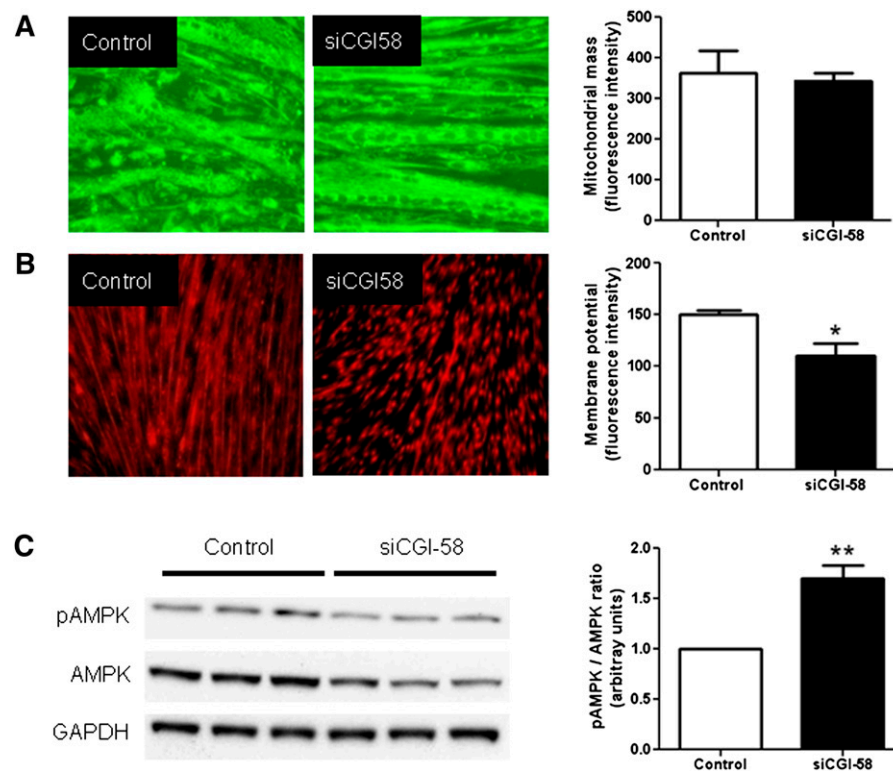
Fig. 5. CGI-58 silencing induces a cellular energy deficit. A: Mitochondrial mass was determined in control myotubes (left panel) and myotubes knocked down for CGI-58 (siCGI58) (middle panel) using the Mitotracker Green FM (20×). Quantitative bar graph of the fluorescence intensity signal (right panel) (n = 4). B: Mitochondrial membrane potential was determined in control myotubes (left panel) and myotubes knocked down for CGI-58 (siCGI58) (middle panel) using the Mitotracker Red CMX-Ros (10×). Quantitative bar graph of the fluorescence intensity signal (right panel) (n = 4). C: Representative blot (left panel) and quantitative bar graph (right panel) of phosphoAMPK to AMPK ratio in control myotubes (left panel) and myotubes knocked down for CGI-58 (siCGI58) (n = 5). Paired Student's t-test * $P < 0.05$, ** $P < 0.01$ versus control.

induces TAGH activity in human *vastus lateralis* muscle lysates, highlighting the limiting role of CGI-58 in this tissue. These data are in agreement with other reports (33). Interestingly, rhCGI-58 failed to induce TAGH in human subcutaneous adipose tissue and this suggests that ATGL may operate nearly maximally in human adipose tissue. This finding is consistent with a recent report showing that adipose-specific overexpression of CGI-58 fails to induce lipolysis in mice and suggests that CGI-58 is not limiting for adipose tissue lipolysis (34). ATGL and CGI-58 may interact at the surface of intramyocellular lipid droplets with lipid coat protein of the perilipin family to provide FA substrates for mitochondrial β-oxidation. Indeed, it was recently shown by Granneman et al. (35) that both CGI-58 and ATGL interacts with perilipin 5 (PLIN5, also called OXPAT or LSDP5) at the surface of the lipid droplet. The authors demonstrated that ATGL activity is strongly deficient in cells expressing PLIN5 mutant proteins able to bind CGI-58 but unable to bind ATGL (35). Thus PLIN5 was shown to be abundantly expressed in oxidative tissues such as skeletal muscle (36). Future studies will be required to unravel the molecular mechanisms regulating the interaction between ATGL, CGI-58, and PLIN5 in the control of lipolysis in skeletal muscle.

To gain further insight into the role of CGI-58 in skeletal muscle, we overexpressed CGI-58 in human primary myotubes. As expected, overexpression of CGI-58 induced TAGH activity and lipolysis as reflected by a reduced TAG content. Elevated CGI-58 protein expression induced a downregulation of ATGL protein expression. This observation suggests that CGI-58 and ATGL may be reciprocally regulated in skeletal muscle and possibly other tissues. Similar findings have been observed in a human white adipocyte cell model (37). This regulation could take place at the transcriptional level because CGI-58 knockdown was accompanied by a significant upregulation of ATGL gene expression. The transcription factor coordinating CGI-58 and ATGL expression is currently unknown. Consistent with an increased lipolytic rate, CGI-58 overexpression reduced the incorporation of oleate into TAG and increased FA release. CGI-58 specifically promoted the oxidation of IMTG-derived FA through increased intracellular FA release. Together, these data suggest that CGI-58-mediated IMTG hydrolysis provides FA substrates for mitochondrial β-oxidation. Conversely, CGI-58 knockdown increased the incorporation of the tracer into TAG reflecting a profound downregulation of TAG hydrolysis and lipolytic flux. Consistently, the reduced lipolytic rate was reflected by a reduced
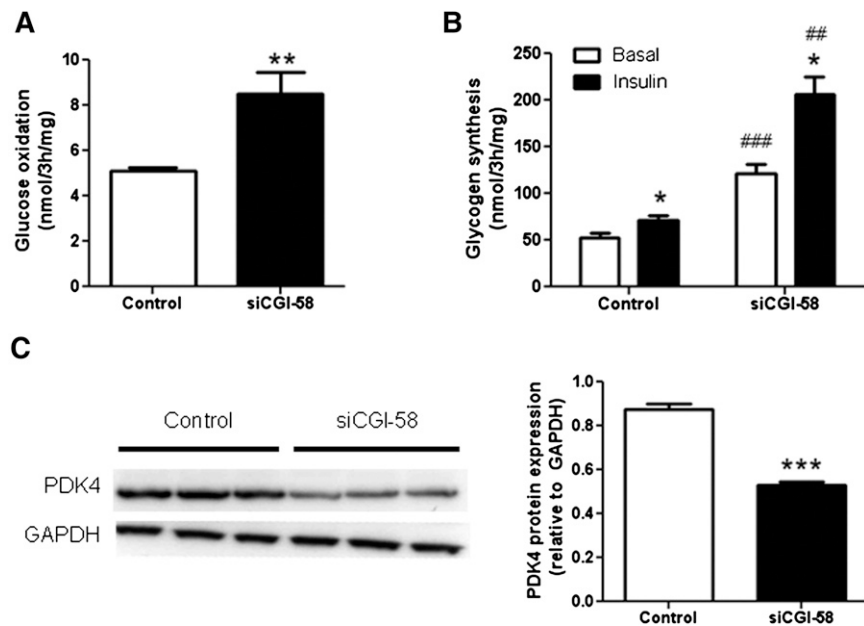
Fig. 6. CGI-58 silencing favors glucose metabolism. A: Basal glucose oxidation was measured in control myotubes and myotubes knocked down for CGI-58 (siCGI58). B: Glycogen synthesis was measured in absence (open bars) or presence (black bars) of 100 nM insulin. * $P < 0.05$, ** $P < 0.01$ versus basal; [##] $P < 0.01$, [###] $P < 0.001$ versus respective control (n = 6). C: Representative blot (left panel) and quantitative bar graph (right panel) of PDK4 protein in control myotubes and myotubes knocked down for CGI-58 (siCGI58) (n = 6), paired Student's *t*-test *** $P < 0.001$ versus control.

incorporation of the tracer into downstream lipolytic products such as DAG, MAG, and FA. Importantly, CGI-58 knockdown was associated with a robust downregulation of IMTG-derived FA oxidation. This effect is partly determined by the reduced intracellular FA release. Collectively, these data point toward a major limiting role of CGI-58 in the regulation of IMTG lipolysis and FA oxidation in human skeletal muscle. The data suggest that although ATGL is an important effector enzyme of lipolysis in skeletal muscle, ATGL cannot operate maximally without its coactivator CGI-58. These data also support the concept that increasing skeletal muscle lipolysis may favor mitochondrial FA oxidation.

Because the suppression of FA oxidation consecutive to CGI-58 knockdown exceeded the suppression of FA release, we sought to investigate whether CGI-58 deficiency altered mitochondrial activity. We could show that CGI-58 deficiency in myotubes reduced mitochondrial membrane potential independently of measurable changes in mitochondrial mass and DNA content. This result is consistent with a robust drop in mitochondrial FA oxidation and apparently not entirely compensated by other energy sources. This observed energy deficit induced AMPK activation, a cellular energy-sensor sensitive to the drop of ADP/ATP ratio (38). Interestingly, CGI-58 deficiency enhanced glucose nonoxidative and oxidative metabolism. The increase in basal glycogen synthesis may reflect a higher basal glucose transport induced by AMPK. Thus, consistent with a reduced incorporation into DAG, insulin-mediated glycogen synthesis tended to increase in siCGI-58 myotubes. These data are also in agreement with a recent study describing a potentially detrimental role of

ATGL activity in human skeletal muscle (12). The rise in glucose oxidation might be the consequence of a classical substrate switch according to the Randle cycle (39). Moreover, this event was associated with a remarkable suppression of PDK4 gene and protein expression. PDK4 is a mitochondrial protein inhibiting glucose oxidation in response to elevated plasma FA availability as observed during fasting or high-fat feeding (40). Thus, the downregulation of PDK4 promotes glucose oxidation. Conversely, CGI-58 overexpression induced FA release, FA oxidation, and PDK4 expression. PDK4 has been reported as a classical PPARδ-target gene (26). We therefore hypothesized that CGI-58-mediated lipolysis provides FA ligands for activating PPARδ in muscle cells. Pioneer studies had shown the ability of PPAR to bind FA such as oleate and arachidonate (41). Thus, this hypothesis is in agreement with a recent study (42), and together they support the view that elevated TAG hydrolysis and the consequential release of FA modulates PPAR transcriptional activity. To test this hypothesis, we first showed that PDK4 expression was highly induced by a selective PPARδ agonist and by oleate in our cell model. This robust induction was completely abolished by a selective PPARδ antagonist. We showed that PDK4 expression can be fully normalized in presence of the PPARδ selective agonist GW0742 during CGI-58 silencing. Additionally, we further demonstrated that the induction of PDK4 by CGI-58 overexpression was totally suppressed by a selective PPARδ antagonist. Together, the data indicate that changes of PDK4 expression in response to changes in CGI-58-mediated lipolysis and FA availability are mediated by PPARδ in skeletal muscle.
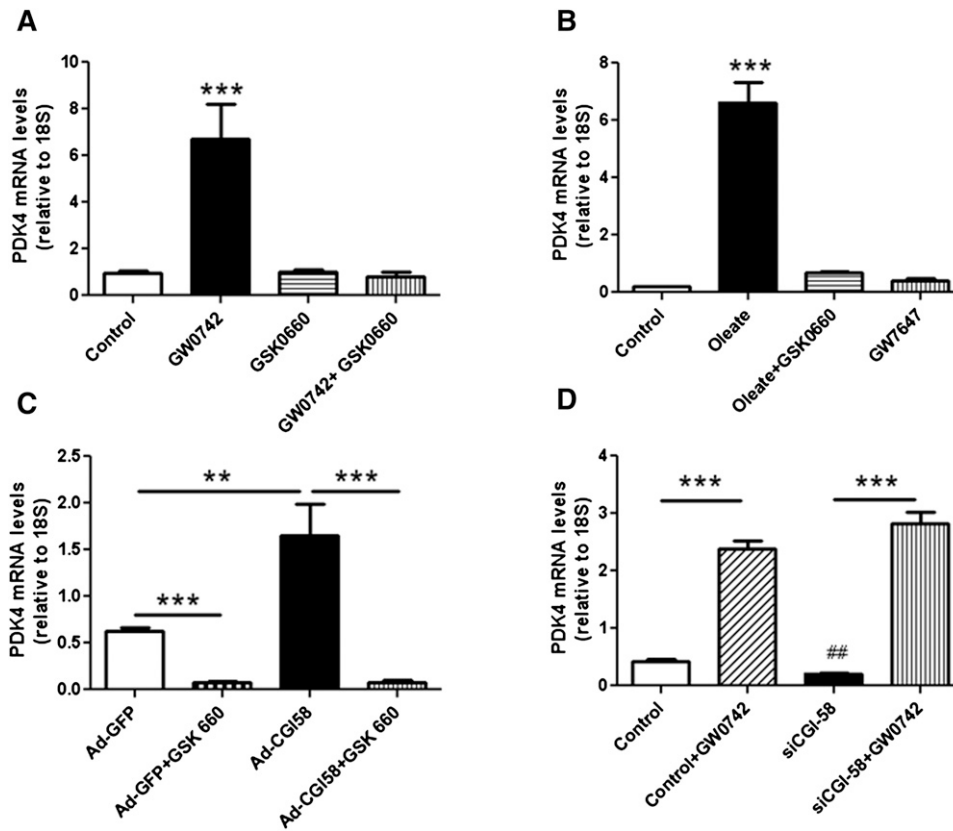
Fig. 7. CGI-58-mediated lipolysis specifically modulates PPARδ-target gene expression. A: PDK4 relative gene expression in myotubes treated for 24 h in absence (control) or presence of the selective PPARδ agonist GW0742 1 nM and the selective PPARδ antagonist GSK0660 500 nM (n = 6); One-way ANOVA *** $P <$ 0.001 versus control. B: PDK4 relative gene expression in myotubes treated for 24 h in absence (control) or presence of 500 µM of oleate alone or in combination with the selective PPARδ antagonist GSK0660 2 µM, and with the selective PPARα agonist GW7647 100 nM (n = 8); One-way ANOVA ***$P <$ 0.001 versus control. C: PDK4 relative gene expression in control myotubes (Ad-GFP) or overexpressing CGI-58 (Ad-CGI58) in absence or presence of the selective PPARδ antagonist GSK0660 500 nM; One-way ANOVA ** $P <$ 0.01, *** $P <$ 0.001 (n = 6). D: PDK4 relative gene expression in control myotubes (Ad-GFP) and myotubes knocked down for CGI-58 (siCGI58) in absence or presence of the selective PPARδ agonist GW0742 1 nM (n = 6), One-way ANOVA, *** $P <$ 0.001 versus GW0742, ## $P <$ 0.01 versus control.

In summary, our data show that CGI-58 is a limiting factor in the regulation of skeletal muscle TAG metabolism and substrate oxidation. Our results are consistent with the view that CGI-58-mediated lipolysis can modulate PPARδ transcriptional activity and the expression of the metabolic switch PDK4. Future studies using animal models with muscle-specific modulations of CGI-58 may help to unravel the specific role of CGI-58 in the regulation of skeletal muscle and whole-body energy metabolism in vivo.

REFERENCES

1. Haemmerle, G., A. Lass, R. Zimmermann, G. Gorkiewicz, C. Meyer, J. Rozman, G. Heldmaier, R. Maier, C. Theussl, S. Eder, et al. 2006. Defective lipolysis and altered energy metabolism in mice lacking adipose triglyceride lipase. *Science.* **312:** 734–737.
2. Zimmermann, R., J. G. Strauss, G. Haemmerle, G. Schoiswohl, R. Birner-Gruenberger, M. Riederer, A. Lass, G. Neuberger, F. Eisenhaber, A. Hermetter, et al. 2004. Fat mobilization in adipose tissue is promoted by adipose triglyceride lipase. *Science.* **306:** 1383–1386.
3. Lass, A., R. Zimmermann, G. Haemmerle, M. Riederer, G. Schoiswohl, M. Schweiger, P. Kienesberger, J. G. Strauss, G. Gorkiewicz, and R. Zechner. 2006. Adipose triglyceride lipase-mediated lipolysis of cellular fat stores is activated by CGI-58 and defective in Chanarin-Dorfman Syndrome. *Cell Metab.* **3:** 309–319.
4. Lefevre, C., F. Jobard, F. Caux, B. Bouadjar, A. Karaduman, R. Heilig, H. Lakhdar, A. Wollenberg, J. L. Verret, J. Weissenbach, et al. 2001. Mutations in CGI-58, the gene encoding a new protein of the esterase/lipase/thioesterase subfamily, in Chanarin-Dorfman syndrome. *Am. J. Hum. Genet.* **69:** 1002–1012.
5. Radner, F. P., S. Grond, G. Haemmerle, A. Lass, and R. Zechner. 2011. Fat in the skin: triacylglycerol metabolism in keratinocytes and its role in the development of neutral lipid storage disease. *Dermatoendocrinol.* **3:** 77–83.
6. Granneman, J. G., H. P. Moore, R. L. Granneman, A. S. Greenberg, M. S. Obin, and Z. Zhu. 2007. Analysis of lipolytic protein trafficking and interactions in adipocytes. *J. Biol. Chem.* **282:** 5726–5735.
7. Watt, M. J., G. J. Heigenhauser, M. O'Neill, and L. L. Spriet. 2003. Hormone-sensitive lipase activity and fatty acyl-CoA content in human skeletal muscle during prolonged exercise. *J. Appl. Physiol.* **95:** 314–321.
8. Watt, M. J., and L. L. Spriet. 2004. Regulation and role of hormone-sensitive lipase activity in human skeletal muscle. *Proc. Nutr. Soc.* **63:** 315–322.
9. Haemmerle, G., R. Zimmermann, M. Hayn, C. Theussl, G. Waeg, E. Wagner, W. Sattler, T. M. Magin, E. F. Wagner, and R. Zechner.

2002. Hormone-sensitive lipase deficiency in mice causes diglyceride accumulation in adipose tissue, muscle, and testis. *J. Biol. Chem.* **277:** 4806–4815.

10. Mulder, H., M. Sorhede-Winzell, J. A. Contreras, M. Fex, K. Strom, T. Ploug, H. Galbo, P. Arner, C. Lundberg, F. Sundler, et al. 2003. Hormone-sensitive lipase null mice exhibit signs of impaired insulin sensitivity whereas insulin secretion is intact. *J. Biol. Chem.* **278:** 36380–36388.

11. Jocken, J. W., E. Smit, G. H. Goossens, Y. P. Essers, M. A. van Baak, M. Mensink, W. H. Saris, and E. E. Blaak. 2008. Adipose triglyceride lipase (ATGL) expression in human skeletal muscle is type I (oxidative) fiber specific. *Histochem. Cell Biol.* **129:** 535–538.

12. Badin, P. M., K. Louche, A. Mairal, G. Liebisch, G. Schmitz, A. C. Rustan, S. R. Smith, D. Langin, and C. Moro. 2011. Altered skeletal muscle lipase expression and activity contribute to insulin resistance in humans. *Diabetes.* **60:** 1734–1742.

13. Bergstrom, J. 1975. Percutaneous needle biopsy of skeletal muscle in physiological and clinical research. *Scand. J. Clin. Lab. Invest.* **35:** 609–616.

14. Ukropcova, B., M. McNeil, O. Sereda, L. de Jonge, H. Xie, G. A. Bray, and S. R. Smith. 2005. Dynamic changes in fat oxidation in human primary myocytes mirror metabolic characteristics of the donor. *J. Clin. Invest.* **115:** 1934–1941.

15. Listenberger, L. L., X. Han, S. E. Lewis, S. Cases, R. V. Farese, Jr., D. S. Ory, and J. E. Schaffer. 2003. Triglyceride accumulation protects against fatty acid-induced lipotoxicity. *Proc. Natl. Acad. Sci. USA.* **100:** 3077–3082.

16. Turpin, S. M., G. I. Lancaster, I. Darby, M. A. Febbraio, and M. J. Watt. 2006. Apoptosis in skeletal muscle myotubes is induced by ceramides and is positively related to insulin resistance. *Am. J. Physiol. Endocrinol. Metab.* **291:** E1341–E1350.

17. Brasaemle, D. L., B. Rubin, I. A. Harten, J. Gruia-Gray, A. R. Kimmel, and C. Londos. 2000. Perilipin A increases triacylglycerol storage by decreasing the rate of triacylglycerol hydrolysis. *J. Biol. Chem.* **275:** 38486–38493.

18. Igal, R. A., and R. A. Coleman. 1996. Acylglycerol recycling from triacylglycerol to phospholipid, not lipase activity, is defective in neutral lipid storage disease fibroblasts. *J. Biol. Chem.* **271:** 16644–16651.

19. Moro, C., J. E. Galgani, L. Luu, M. Pasarica, A. Mairal, S. Bajpeyi, G. Schmitz, D. Langin, G. Liebisch, and S. R. Smith. 2009. Influence of gender, obesity, and muscle lipase activity on intramyocellular lipids in sedentary individuals. *J. Clin. Endocrinol. Metab.* **94:** 3440–3447.

20. Folch, J., M. Lees, and G. H. Sloane Stanley. 1957. A simple method for the isolation and purification of total lipides from animal tissues. *J. Biol. Chem.* **226:** 497–509.

21. Morrison, W. R., and L. M. Smith. 1964. Preparation of fatty acid methyl esters and dimethylacetals from lipids with boron fluoride-methanol. *J. Lipid Res.* **5:** 600–608.

22. Bonnard, C., A. Durand, S. Peyrol, E. Chanseaume, M. A. Chauvin, B. Morio, H. Vidal, and J. Rieusset. 2008. Mitochondrial dysfunction results from oxidative stress in the skeletal muscle of diet-induced insulin-resistant mice. *J. Clin. Invest.* **118:** 789–800.

23. Ghosh, A. K., G. Ramakrishnan, C. Chandramohan, and R. Rajasekharan. 2008. CGI-58, the causative gene for Chanarin-Dorfman syndrome, mediates acylation of lysophosphatidic acid. *J. Biol. Chem.* **283:** 24525–24533.

24. Montero-Moran, G., J. M. Caviglia, D. McMahon, A. Rothenberg, V. Subramanian, Z. Xu, S. Lara-Gonzalez, J. Storch, G. M. Carman, and D. L. Brasaemle. 2010. CGI-58/ABHD5 is a coenzyme A-dependent lysophosphatidic acid acyltransferase. *J. Lipid Res.* **51:** 709–719.

25. Pilegaard, H., and P. D. Neufer. 2004. Transcriptional regulation of pyruvate dehydrogenase kinase 4 in skeletal muscle during and after exercise. *Proc. Nutr. Soc.* **63:** 221–226.

26. Ehrenborg, E., and A. Krook. 2009. Regulation of skeletal muscle physiology and metabolism by peroxisome proliferator-activated receptor delta. *Pharmacol. Rev.* **61:** 373–393.

27. DeFronzo, R. A. 2004. Pathogenesis of type 2 diabetes mellitus. *Med. Clin. North Am.* **88:** 787–835 (ix.).

28. McGarry, J. D. 2002. Banting lecture 2001: dysregulation of fatty acid metabolism in the etiology of type 2 diabetes. *Diabetes.* **51:** 7–18.

29. Krssak, M., K. Falk Petersen, A. Dresner, L. DiPietro, S. M. Vogel, D. L. Rothman, M. Roden, and G. I. Shulman. 1999. Intramyocellular lipid concentrations are correlated with insulin sensitivity in humans: a 1H NMR spectroscopy study. *Diabetologia.* **42:** 113–116.

30. Pan, D. A., S. Lillioja, A. D. Kriketos, M. R. Milner, L. A. Baur, C. Bogardus, A. B. Jenkins, and L. H. Storlien. 1997. Skeletal muscle triglyceride levels are inversely related to insulin action. *Diabetes.* **46:** 983–988.

31. Perseghin, G., P. Scifo, F. De Cobelli, E. Pagliato, A. Battezzati, C. Arcelloni, A. Vanzulli, G. Testolin, G. Pozza, A. Del Maschio, et al. 1999. Intramyocellular triglyceride content is a determinant of in vivo insulin resistance in humans: a 1H–13C nuclear magnetic resonance spectroscopy assessment in offspring of type 2 diabetic parents. *Diabetes.* **48:** 1600–1606.

32. Langfort, J., T. Ploug, J. Ihlemann, M. Saldo, C. Holm, and H. Galbo. 1999. Expression of hormone-sensitive lipase and its regulation by adrenaline in skeletal muscle. *Biochem. J.* **340:** 459–465.

33. Alsted, T. J., L. Nybo, M. Schweiger, C. Fledelius, P. Jacobsen, R. Zimmermann, R. Zechner, and B. Kiens. 2009. Adipose triglyceride lipase in human skeletal muscle is upregulated by exercise training. *Am. J. Physiol. Endocrinol. Metab.* **296:** E445–E453.

34. Caviglia, J. M., J. L. Betters, D. H. Dapito, C. C. Lord, S. Sullivan, S. Chua, T. Yin, A. Sekowski, H. Mu, L. Shapiro, et al. 2011. Adipose-selective overexpression of ABHD5/CGI-58 does not increase lipolysis or protect against diet-induced obesity. *J. Lipid Res.* **52:** 2032–2042.

35. Granneman, J. G., H. P. Moore, E. P. Mottillo, Z. Zhu, and L. Zhou. 2011. Interactions of perilipin-5 (Plin5) with adipose triglyceride lipase. *J. Biol. Chem.* **286:** 5126–5135.

36. Wolins, N. E., B. K. Quaynor, J. R. Skinner, A. Tzekov, M. A. Croce, M. C. Gropler, V. Varma, A. Yao-Borengasser, N. Rasouli, P. A. Kern, et al. 2006. OXPAT/PAT-1 is a PPAR-induced lipid droplet protein that promotes fatty acid utilization. *Diabetes.* **55:** 3418–3428.

37. Bezaire, V., A. Mairal, C. Ribet, C. Lefort, A. Girousse, J. Jocken, J. Laurencikiene, R. Anesia, A. M. Rodriguez, M. Ryden, et al. 2009. Contribution of adipose triglyceride lipase and hormone-sensitive lipase to lipolysis in hMADS adipocytes. *J. Biol. Chem.* **284:** 18282–18291.

38. Hardie, D. G. 2007. AMP-activated/SNF1 protein kinases: conserved guardians of cellular energy. *Nat. Rev. Mol. Cell Biol.* **8:** 774–785.

39. Randle, P. J., P. B. Garland, C. N. Hales, and E. A. Newsholme. 1963. The glucose fatty-acid cycle. Its role in insulin sensitivity and the metabolic disturbances of diabetes mellitus. *Lancet.* **1:** 785–789.

40. Spriet, L. L., R. J. Tunstall, M. J. Watt, K. A. Mehan, M. Hargreaves, and D. Cameron-Smith. 2004. Pyruvate dehydrogenase activation and kinase expression in human skeletal muscle during fasting. *J. Appl. Physiol.* **96:** 2082–2087.

41. Schmidt, A., N. Endo, S. J. Rutledge, R. Vogel, D. Shinar, and G. A. Rodan. 1992. Identification of a new member of the steroid hormone receptor superfamily that is activated by a peroxisome proliferator and fatty acids. *Mol. Endocrinol.* **6:** 1634–1641.

42. Sapiro, J. M., M. T. Mashek, A. S. Greenberg, and D. G. Mashek. 2009. Hepatic triacylglycerol hydrolysis regulates peroxisome proliferator-activated receptor alpha activity. *J. Lipid Res.* **50:** 1621–1629.